High-resolution pulsed field ionization study of high Rydberg states of benzene

ARTICLE *in* JOURNAL OF MOLECULAR STRUCTURE · DECEMBER 2001

Impact Factor: 1.6 · DOI: 10.1016/S0022-2860(01)00849-3

3 AUTHORS, INCLUDING:

Andreas Osterwalder
École Polytechnique Fédérale de Laus...
36 PUBLICATIONS **561** CITATIONS
SEE PROFILE

Stefan Willitsch
University of Basel
51 PUBLICATIONS **730** CITATIONS
SEE PROFILE

ELSEVIER

Journal of Molecular Structure 599 (2001) 163–176

Journal of
MOLECULAR
STRUCTURE

www.elsevier.com/locate/molstruc

High-resolution pulsed field ionization study of high Rydberg states of benzene ☆

A. Osterwalder, S. Willitsch, F. Merkt*

Laboratorium für Physikalische Chemie, ETH Zürich, CH-8092 Zürich, Switzerland

Received 20 July 2000; accepted 30 October 2000

Abstract

The influence of dc electric fields and ion concentrations on the long-term stability of high Rydberg states of benzene has been studied by delayed pulsed field ionization and millimeter wave spectroscopy following resonance-enhanced two-photon excitation via selected rotational levels of the $|S_1 6^1\rangle$ intermediate state. The long-term stability, which is probed by applying pulsed electric fields at delay times of more than 1 μs after photoexcitation, originates from Stark mixing of weakly penetrating series, presumably g series, with quantum defect of approximately 0.003 with nonpenetrating high-ℓ states. The pulsed field ionization yield is strongly influenced by the experimental conditions and is characterized by a marked dependence on the principal quantum number n. At n values beyond 100, the weak stray electric fields in the apparatus are sufficient to stabilize an important fraction of the optically accessible Rydberg states by Stark mixing. In the range $n = 40$–80, long-term stability beyond 1 μs cannot be achieved by Stark mixing induced by homogeneous dc electric fields but can be attained by generating a sufficient concentration of ions in the experimental volume. A simple rule (c/(ions/cm^3) $\geq (9.14 \times 10^{15}|\mu_i|/n^5)^{3/2}$) is derived that relates the minimum ion concentration required to induce long-term stability to the principal quantum number and the quantum defect of the optically accessible Rydberg states. Below $n = 40$ long-term stability cannot be induced unless very large ion concentrations beyond 10^8 ions/cm^3 are generated. Spectra of Rydberg states in the range $n = 27$–40 can nevertheless be recorded at high laser fluence by monitoring the fragmentation products that result from the absorption of one or more photons by the Rydberg molecules. The results enable a quantitative discussion of important features of the new technique of cross-correlation ionization energy spectroscopy (CRIES) recently developed by Neuhauser et al., (J. Chem. Phys. 106 (1997) 896). In particular, we show that (1) the technique only works because of Stark mixing of at least one of the optically accessible series with nonpenetrating high-ℓ states induced by weak electric fields, (2) this series must possess a quantum defect significantly smaller than 0.1 and an orbital angular momentum quantum number $\ell \geq 3$, (3) significant n-dependent energy shifts in the position of the Rydberg states induced by electric fields can introduce systematic errors in the extrapolation of the series limits.

Keywords: Field ionization; Benzene; High Rydberg states; Millimetre wave spectroscopy; ZEKE spectroscopy

1. Introduction

In a recent series of articles, Neusser and co-workers [1–6] have demonstrated that high Rydberg states of benzene and of van der Waals complexes of rare gas atoms with benzene and substituted benzene rings can be studied spectroscopically at high resolution by

☆ This paper is dedicated to Professor Alfred Bauder in appreciation of his significant contributions to the field of microwave spectroscopy.

* Corresponding author. Tel.: +41-1-632-4367; fax: +41-1-632-1021.

E-mail address: merkt@xuv.phys.chem.ethz.ch (F. Merkt).

0022-2860/01/$ - see front matter
PII: S0022-2860(01)00849-3

delayed pulsed field ionization following a $(1 + 1')$ two-photon excitation via the $|S_1 6^1\rangle$ intermediate state using two near-Fourier-transform-limited nanosecond pulsed dye lasers. Important observations made during these studies are that (1) well-resolved transitions to Rydberg states in the range of principal quantum number between $n = 40$ and $n = 130$ can be recorded, (2) the linewidths of the transitions range between 400 MHz and approximately 1 GHz and are significantly broader than the laser bandwidth of better than 70 MHz, (3) most of the high Rydberg states probed experimentally have long lifetimes up to several microseconds although, in some experiments, the field ionization pulse was applied immediately (i.e. 10–30 ns) after the laser pulse [1,2,4,5], (4) the observed Rydberg states have vanishing quantum defects, and (5) the Rydberg series are not affected by any perturbation. Observations (4) and (5) imply that the Rydberg series can be extrapolated in a straightforward way to obtain the series limits, i.e. the positions of ionic energy levels with respect to the selected intermediate state, with a precision limited solely by the width of the observed lines. To efficiently extract this information, a cross-correlation analysis of the experimental spectra was implemented which enables the conversion of the Rydberg spectra into cross-correlation ionization energy spectra (CRIES) [1,2]. In the following we use the acronym CRIES introduced by Neuhauser et al. [2] to designate the overall procedure that consists of measuring high-resolution Rydberg spectra and subsequently processing them to obtain high-resolution cation spectra and precise ionization energies.

Clearly these studies represent a breakthrough in cation spectroscopy and enable the measurements of spectra at a resolution approaching that that can be reached in the electronic ground state of the parent neutral species which, in the case of benzene and benzene–rare gas clusters, were studied in detail by Bauder and his group using microwave spectroscopy [7–10]. At the same time, the experimental observations depart significantly from the known behavior of the optically accessible low-ℓ Rydberg states of small molecular systems that usually have nonzero quantum defects and are short lived. In addition, the Rydberg spectra of small molecules show many strong perturbations that severely complicate the analysis and the determination of the series limits [11,12].

In order to explain their results, Neusser and co-workers invoked the same reasons as those that are used to explain the long lifetimes of the Rydberg states probed by PFI-ZEKE photoelectron spectroscopy, namely that the states probed by pulsed field ionization are Stark states arising from the mixing of the optically accessible Rydberg states with nonpenetrating Rydberg states of higher orbital angular momentum induced by small stray electric fields [13–19]. The small electric fields responsible for the mixing are difficult to control experimentally and are usually guessed. They were reported to be typically 40 mV/cm in the initial study of benzene [1] and less than 30 mV/cm in later studies [2,4]. In the case of benzene, it was suggested that the optically accessible g or i states might be long-lived enough to survive the several microseconds separating photoexcitation and delayed pulsed field ionization [20].

The impressive quality of the data obtained by Neusser and co-workers was an incentive for us to find out whether and, if so, under which conditions, their method can be generally applied to other molecules. We have initially chosen the benzene molecule because it enabled a direct comparison with previous studies of its high Rydberg states by delayed pulsed field ionization [21–25,1,2]. The spectroscopic and dynamical properties of lower Rydberg states of benzene have been well studied [26–31]. These states decay by rapid internal conversion on a sub-picosecond timescale. Chupka [32] has discussed the implication of the studies of low n Rydberg states for the decay behavior of the high n states probed by PFI-ZEKE photoelectron spectroscopy. Our hope at the start of these investigations was that some of the optically accessible Rydberg states of benzene, in particular the g or the i states, would be sufficiently long-lived (as suggested by Neusser [20]) to enable the recording of millimeter wave spectra of benzene Rydberg states at the sub-MHz resolution we have recently achieved in our studies of argon [33], krypton [34,35] and H_2 [36] Rydberg states.

The laser system used in the present work only allowed a resolution of slightly better than 2 GHz, i.e. a factor of five worse than the narrowest lines observed by Neuhauser, Siglow and Neusser [2]. This clear disadvantage was compensated by a good control of the stray fields that we can measure accurately by millimeter wave spectroscopy [35] and

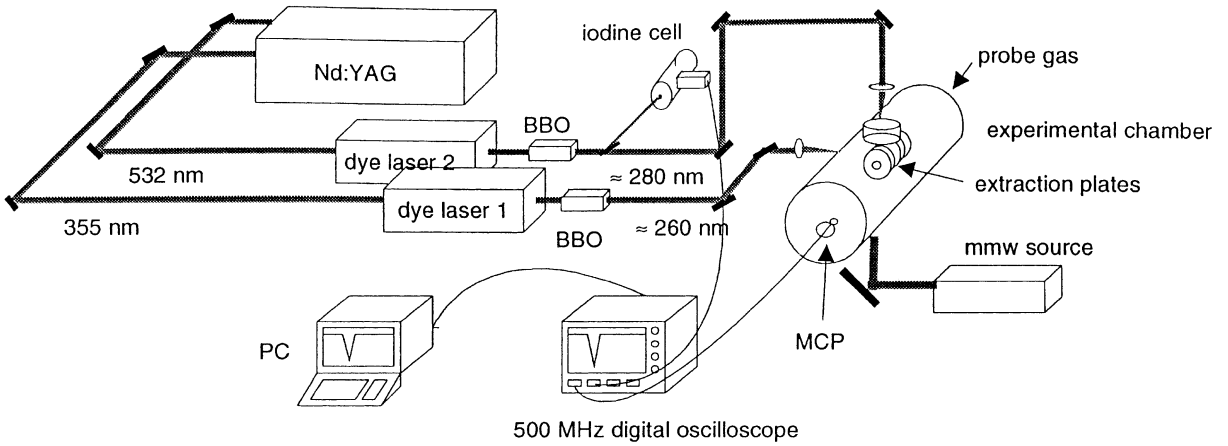

Fig. 1. Schematic view of the experimental setup.

maintain to a level below 1 mV/cm. The use of millimeter wave spectroscopy also enabled us to record spectra of transitions between high Rydberg states of benzene with linewidths as narrow as 70 MHz, i.e. almost one order of magnitude better than that obtained in the laser experiments. Our study complements the study of Neusser and co-workers in that it quantifies the role played by weak homogeneous stray fields on the observed spectra and demonstrates the necessity to create sufficient concentrations of ions to observe long-lived (lifetime $\tau \geq 1\ \mu s$) Rydberg states. It also enables us to draw several conclusions on the potential of the technique pioneered by Neusser and co-workers for the study of other molecular systems.

2. Experiment

A schematic view of the experimental set-up is presented in Fig. 1. Two tunable Nd:YAG pumped dye lasers are used to excite benzene molecules from the ground state $|S_0\rangle$ to high Rydberg states located below the lowest ionization threshold via a selected rotational level, the $|J' = 2, K' = 2, +l\rangle$ level, of the $|S_1 6^1\rangle$ intermediate state. This $(1 + 1')$ resonance-enhanced two-photon excitation sequence has been used in several earlier studies of the threshold photoionization of benzene [21–25,1,2].

The first laser, operated with Coumarin 307 dye, is pumped by the tripled output (355 nm) of a pulsed Nd:YAG laser (repetition rate 10 Hz, pulse length ≈ 7 ns) and is frequency doubled in a BBO crystal to induce transitions from the ground state to the $|S_1 6^1\rangle$ intermediate state. The second dye laser, operated with Fluorescein 27 dye, is pumped by the second harmonic (532 nm) of the Nd:YAG laser and is also frequency doubled in a BBO crystal. This laser further excites the benzene molecules from the selected intermediate level to high Rydberg states. Both lasers are operated with intracavity etalons and the bandwidth of the UV radiation, estimated from the full width at half maximum (FWHM) of observed transitions, amounts to less than 0.06 cm^{-1} (2 GHz). The UV output of the first laser can be attenuated from 200 μJ/pulse to less than 1 μJ/pulse. The second laser was operated at a constant energy of ≈ 1 mJ/pulse in the UV.

The two laser beams intersect a skimmed supersonic expansion of a mixture of 2% benzene in neon (nozzle stagnation pressure of 2.5 bar) in the middle of the experimental chamber. At the crossing point, all three beams propagate perpendicularly to each other and the supersonic expansion has a diameter of 1–2 mm. During operation of the pulsed nozzle the background pressure in the experimental chamber rises from 10^{-7} to 3×10^{-7} mbar. The expansion conditions were optimized so as to minimize the formation of clusters in the molecular beam.

The diameter of the laser beams in the photoexcitation region amounts to 3 mm and 6 mm for the first and second laser, respectively. In experiments for which high fluences are required, the laser beams can be focused into the molecular beam. Optimal sensitivity is achieved when the first laser is focused cylindrically so that the focal line lies parallel to the propagation axis of the second laser that is focused spherically. The width and length of the focal line of the first laser are estimated to be approximately 200 μm and 3 mm, respectively.

The photoexcitation region has been designed to minimize external perturbations caused by stray fields. It consists of a set of five cylindrically symmetric polished extraction plates separated by 1.5 cm and is surrounded by a double layer of mumetal tubing to ensure magnetic shielding. Under conditions of normal operation, the stray fields present in the photoexcitation volume, which can be measured spectroscopically as explained in Refs. [33,35], do not exceed 1 mV/cm.

Long-lived high Rydberg states are detected by delayed pulsed field ionization (PFI) using electric fields of −45 V/cm to −260 V/cm and delay times of typically 2.5 μs. The pulsed electric fields also serve the purpose of extracting the electrons towards a microchannel plate (MCP) detector. The MCP signals are displayed and processed on a 500 MHz digital oscilloscope and the data are transferred to a PC. Absolute calibration of the dye laser fundamental wavenumbers is derived from simultaneous measurement of I_2 laser induced fluorescence spectra and making reference to the iodine atlas [37].

The concentration of $C_6H_6^+$ ions in the photoexcitation volume is varied by adjusting the fluence of the first laser. Increasing the fluence results in a rapid increase of the one color (1 + 1) resonance-enhanced multiphoton ionization (REMPI) signal. At the highest fluences, when considerable amounts of ions (10^8 ions/cm^3 and beyond) are produced, a spurious electron signal is observed that does not disappear when the second laser is turned off. This undesirable signal originates from electrons that remain trapped in the cloud of ions generated by the first laser. These electrons only get released when the delayed pulsed electric field is applied. To remove these unwanted electrons a pulsed field of +1 V/cm and 400 ns duration is applied before the field ionization pulse.

The resolution of the laser experiments is limited by the 0.06 cm^{-1} bandwidth of the second laser. To obtain spectroscopic information at higher resolution, millimeter waves are used to record spectra of transitions from the Rydberg states prepared in the (1 + 1′) two-photon absorption process described above to higher lying Rydberg states. In these experiments care must be taken to selectively ionize the final state of the millimeter wave transitions as explained in Ref. [33]. The millimeter waves are directed into the experimental chamber from below in a counterpropagating arrangement with respect to the second laser. The maximum resolution of the millimeter wave spectra is determined by the measurement time, i.e. the time between the laser pulse and the pulsed ionization field and can be as high as 60 kHz [35].

3. Results

3.1. Measurements at low laser fluences

In a first series of measurements the lasers were operated at low fluence, i.e. they were not focused into the excitation region. A pulsed electric field of −45 V/cm was applied, which is sufficient to cause the diabatic field ionization of Rydberg states down to $n \approx 64$ [13,38].

Fig. 2 shows a series of spectra recorded in the presence of dc electric fields with field strength ranging from 0 mV/cm (lowest trace) to 50 mV/cm (top trace). The fluence of the first laser was held constant at 400 μJ/cm^2 and the delay time between photoexcitation and pulsed field ionization amounted to 2.5 μs. Contrary to our expectations, a decrease of signal intensities is observed with increasing field strength. We had indeed anticipated that ℓ-mixing induced by the 50 mV/cm dc field would lead to a lengthening of the lifetimes of the Rydberg states probed experimentally and thus to an enhancement of the delayed pulsed field ionization signal, at least on its low frequency side. The behavior observed in Fig. 2 is reminiscent of observations made at high n values by PFI-ZEKE photoelectron spectroscopy in NO [39], argon [40] and benzene [41,17] where intentionally applied dc electric fields caused a reduction of the pulsed field ionization signal.

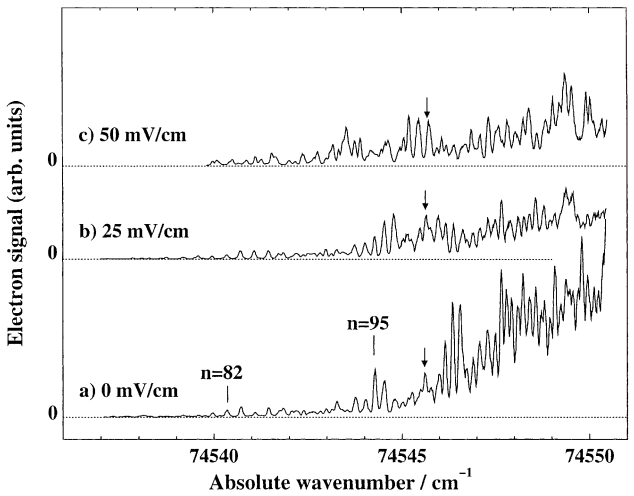

Fig. 2. The effect of dc electric fields on the delayed pulsed field ionization spectrum of benzene recorded at a laser fluence of 400 μJ/cm^2. Traces b and c were recorded at an electric field strength of 25 mV/cm and 58 mV/cm, respectively. The stray field present during the recording of Trace a amounted to less than 1 mV/cm. The vertical scale has been normalized at the position of the vertical arrow.

Varying the fluence of the first laser also modifies the appearance of the PFI spectra as is illustrated in Fig. 3 that shows three spectra recorded at three different fluences between 35 mV/cm (lowest trace) and 400 μJ/cm^2 (top trace) at a dc field strength of 50 mV/cm. For direct comparison of the intensities, the spectra were normalized by dividing by the fluence of the first laser. A fluence of 35 μJ/cm^2 corresponds to conditions where the formation of benzene cations by the one-color two-photon ionization process is strongly reduced. The reproducibility of spectra recorded under conditions of very low fluences (below 100 μJ/cm^2) of the first laser is poor and spectral features appear at random.

The dependence of the spectra from the delay time

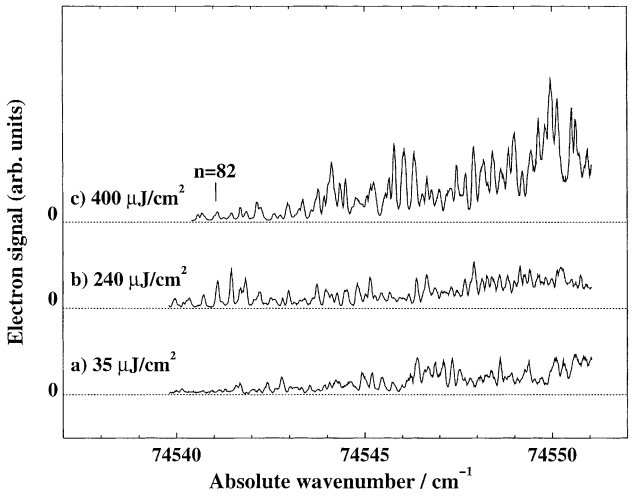

Fig. 3. The effect of the fluence of the first laser on the delayed pulsed field ionization spectrum of benzene (lasers not focussed). Traces a, b and c were recorded at a fluence of 35 μJ/cm^2, 240 μJ/cm^2 and 400 μJ/cm^2, respectively. The vertical scale has been normalized by dividing by the fluence of the first laser.

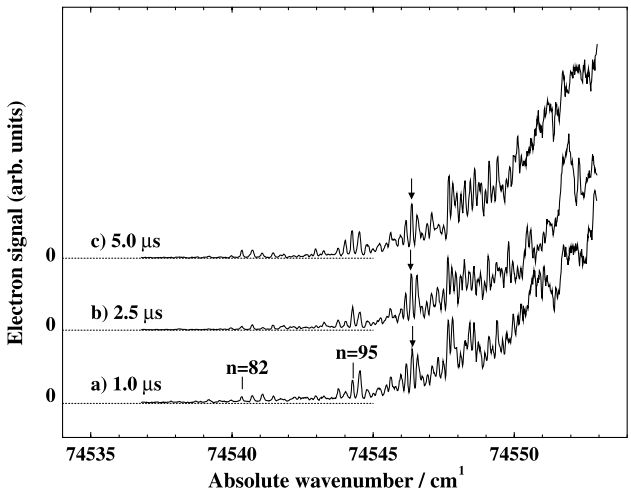

Fig. 4. The effect of the delay time between photoexcitation and pulsed field ionization on the delayed pulsed field ionization spectrum of benzene. Traces a, b and c were recorded at a delay time of 1.0, 2.5 and 5 μs, respectively. The vertical scale has been normalized at the position of the vertical arrow.

between excitation and field ionization is displayed in Fig. 4. Although delay times were varied, at a constant fluence of 400 μJ/cm^2 of the first laser, by a factor of 5 from 1 μs (Trace a) to 5 μs (Trace c), no significant changes in the spectra are noticeable.

These results at low laser fluences can be summarized as follows:

1. Signal intensities, structural wealth and reproducibility of the spectra increase rapidly with increasing fluence of the first laser.
2. Rydberg states below $n \approx 80$ are not observed which suggests that they decay completely before the pulsed field is applied.
3. Application of external dc fields causes a decrease of signal intensities at all n values probed experimentally.
4. The Rydberg states that survive 1 μs after

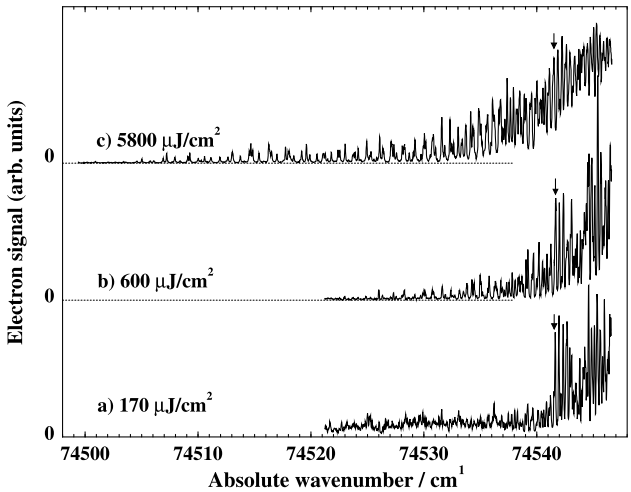

Fig. 5. Pulsed field ionization spectra of high Rydberg state of benzene recorded with the laser beams focused in the experimental volume. Traces a, b and c correspond to an estimated fluence of 170 μJ/cm^2, 600 μJ/cm^2 and 5.8 mJ/cm^2, respectively. The vertical scale has been normalized at the position of the vertical arrow.

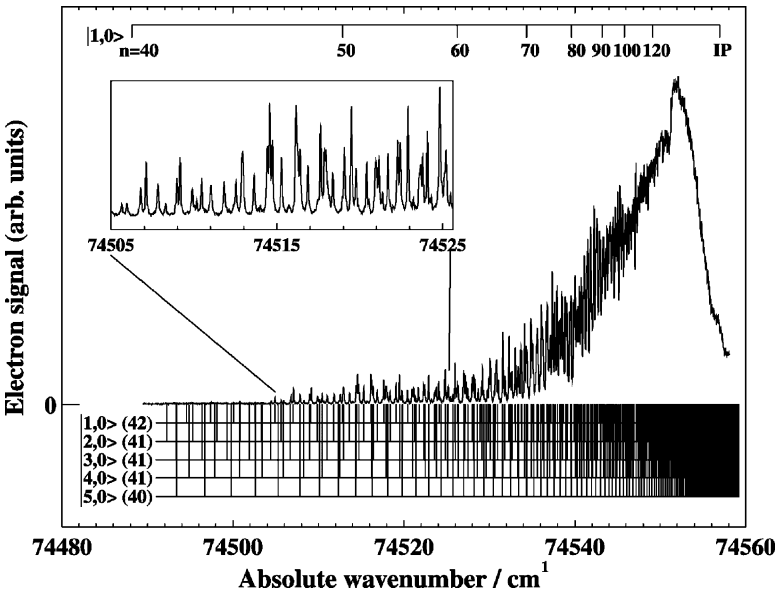

Fig. 6. The delayed pulsed field ionization spectrum of benzene recorded at a fluence of 5.8 mJ/cm^2. The assignment bars indicate the Rydberg series that converge to the $|J^+, K^+\rangle$ rotational levels of the cation. The number in parenthesis next to the $|J^+, K^+\rangle$ label represents the principal quantum number n of the lowest Rydberg state of each series that is marked along the assignment bar. The inset represents an enlarged view of the middle part of the spectrum in the range of n values between 45 and 55.

photoexcitation do not show any decay up to delay times beyond 5 μs. However, these long-lived Rydberg states only represent a fraction of the total signal at threshold. A large fraction of the optically prepared states therefore decays during the first microsecond.

3.2. Measurements at high laser fluence

In a further series of measurements, the lasers were focused into the excitation region. In order not to reduce the excitation volume too much and thus sacrifice the sensitivity, a cylindrical focus with an estimated diameter of approximately 200 μm was employed for the first laser. The pulsed electric field used for field ionization was increased to −260 V/cm so that the diabatic field ionization of Rydberg states with n as low as 40 could be observed. The electric field pulse was applied 2.5 μs after excitation.

The dependence of the spectral features on the laser fluence is illustrated in Fig. 5. By increasing it from approximately 170 μJ/cm^2 to 5.8 mJ/cm^2, one observes a large shift of the onset of the field ionization signal to lower n values. The onset is at around $n = 80$ at the lowest fluence (Trace a), $n = 60$ at the intermediate fluence (Trace b) and $n = 40$ at the highest fluence (Trace c).

The concentration of prompt ions in the excitation volume increases from approximately 10^6 ions/cm^3 (Fig. 5a) to approximately 10^8 ions/cm^3 (Fig. 5c), a value that is inferred from the ion signal intensities and our estimated focal volume. Because of the uncertainty in the focal volume, these ion concentrations are only expected to give the correct order of magnitude. The ion concentration corresponding to the fluence used to record the spectrum in Fig. 5a was estimated independently to be 5×10^5 ions/cm^3 from a measurement of the linewidths of transitions recorded by millimeter wave spectroscopy (see below). At the high ion concentration present during the recording of Fig. 5c it is necessary to apply a small pulsed electric field of 1 V/cm to avoid the detection of electrons that are trapped in the ion cloud (see Section 2) and which otherwise lead to an unwanted background signal. The velocity imparted to the ions by the Coulomb repulsion forces at these high ion concentrations also exceeds typical relative velocities

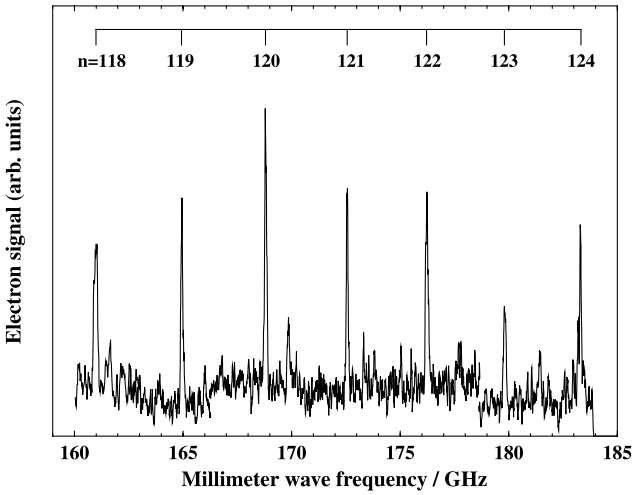

Fig. 7. Millimeter wave spectrum of benzene showing transitions from $n = 91$ to $n = 118$–124 Rydberg states.

of the neutral particles in the cold supersonic expansion.

Fig. 5c is displayed on a larger scale in Fig. 6 with assignment of the observed Rydberg series. The spectrum reveals a rich spectral structure that starts with a very weak signal in the range $n = 40$–45. All observed features can be accounted for by five Rydberg series of approximately zero quantum defect that converge on the $|J^+, K^+\rangle = |1,0\rangle$, $|2,0\rangle$, $|3,0\rangle$, $|4,0\rangle$ and $|5,0\rangle$ rotational states of the vibronic ground state of the cation.

These results at high laser fluences and high ion concentrations can be summarized as follows:

1. The trend, already noticed at low fluences, that signal intensities and spectral complexity increase with the fluence of the first laser continues to manifest itself.
2. The reproducibility of the spectra becomes excellent at high fluence.
3. Rydberg states down to $n \approx 40$ contribute to the spectra. The agreement between the measured series with the computed series displayed along the assignment bars in Fig. 6 and the series observed by Neusser and co-workers [2,3] is excellent, both as far as line intensities and positions are concerned, and our analysis supports their values for the ionization limits and the quantum defects.
4. Application of small external dc fields (up to 200 mV/cm) leads to a decrease of signal intensity at all n values probed experimentally.

3.3. UV–UV–millimeter waves triple-resonance experiments

Further insights in the spectral and dynamical properties of the high Rydberg states of benzene can be gained from high-resolution UV–UV–millimeter waves triple-resonance experiments. In these experiments, the frequency of the first and second laser is kept fixed so as to excite a selected high Rydberg state and the millimeter waves are scanned to induce transitions to higher Rydberg states. Inhomogeneous electric fields such as those generated by ions in the experimental volume have the undesirable effect of inducing large line broadenings that render the observation of spectral structure very difficult. To avoid the generation of too high a concentration of ions, it was necessary to prepare the initial Rydberg state using low fluences, and the lasers were not focused into the excitation region. Under these conditions, only Rydberg states with $n > 80$ are sufficiently long-lived to be observed by delayed pulsed field ionization (see Figs. 2–4). Fig. 7 shows a millimeter wave spectrum of transitions between $n = 91$ and $n = 118$–124 Rydberg states of benzene. The spectrum was

recorded by monitoring the field ionization signal induced by a pulsed field of −9 V/cm applied 7.5 μs after the laser pulse. Unlike what we observed in Ar [33], Kr [35] and H_2 [36], where millimeter waves transitions between $n = 90$ and 125 are easily observable at low millimeter wave intensities (30 dB attenuation, corresponding to intensities of $\approx 0.5\ \mu W/cm^2$), much higher intensities (4 dB attenuation, corresponding to intensities of $\approx 200\ \mu W/cm^2$) were necessary to observe any signal at all in benzene.

The millimeter wave spectrum reveals one series of lines with linewidths varying between 70 MHz and 200 MHz (FWHM). These lines are all significantly narrower than the narrowest lines (width of 400 MHz) that could be observed by Neuhauser, Siglow and Neusser [2] in the range $n = 60$–100, but they are considerably broader than the width of 500 kHz or less that can be measured in the millimeter wave spectra of Ar, Kr and H_2 in the same apparatus and the same range of n values. A fit of the line positions to the Rydberg formula yields zero quantum defect within the error boundaries for both the lower and the upper levels of the millimeter wave transitions.

It turned out to be extremely difficult to reproduce these millimeter wave spectra because of their surprisingly pronounced dependence on day-to-day fluctuations in the experimental conditions. Only an extremely narrow range of possible combinations of laser and millimeter wave intensities was compatible with observable millimeter wave spectra.

The investigation of high Rydberg states of benzene by millimeter wave spectroscopy yielded the following additional information:

1. The states involved in the millimeter wave transitions have vanishing quantum defect within the limits of resolution and sensitivity of the measurements.
2. The transitions are only observable at unusually high millimeter wave intensities.
3. The lines are much broader than expected from measurements in other atomic and molecular systems.

These observations suggest that the states involved in the millimeter wave transitions are Stark states and not the optically accessible d and g Rydberg states. The widths of the transitions thus reflect the width of the Stark manifold of high-ℓ ($3n^2F$ in atomic units). From the observed linewidths one can estimate the average electric field present in the experimental volume. At $n = 125$, the measured linewidths of approximately 150 MHz of most transitions in Fig. 7 imply an average electric field of approximately 2.5 mV/cm. This field is largely caused by the ions generated by the laser pulses. Using the formula of Holtsmark [42–44], this average field can therefore be used to estimate an ion concentration of approximately 5×10^5 ions/cm^3.

3.4. Observation of Rydberg states with $n \geq 27$ by detection of ion fragments

Only Rydberg states with $n > 40$ can be observed by delayed pulsed field ionization in Fig. 6. In a recent publication, Siglow and Neusser have successfully obtained spectra at lower values of n (down to $n \approx 37$) by further exciting the Rydberg states during the laser pulse and observing the subsequent autoionization [3]. In contrast to PFI experiments in which only Rydberg states with lifetimes longer than the delay time are detected, Rydberg states with lifetimes comparable with the laser pulse length can be observed in these experiments. In order to record spectra of states with still lower n values it becomes necessary to increase the intensity of the laser pulses so that the absorption of an additional photon effectively competes with the decay, and the lasers must be focused into the excitation region. Under these conditions, we do not only observe a large (1 + 1) two-photon ionization signal but also fragmentation products that originate from the absorption of one or more additional photons by the Rydberg molecules. By monitoring the $C_4H_x^+$ fragment yield as a function of the wavenumber of the second laser we were able to record spectra of Rydberg states with principal quantum numbers as low as $n = 27$ as illustrated in Fig. 8. The advantage of detecting fragments lies in the fact that the background (1 + 1) REMPI ionization signal from the first laser,

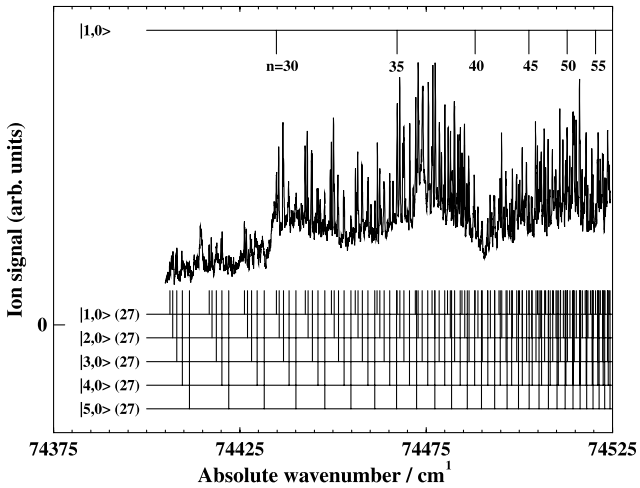

Fig. 8. Spectrum of Rydberg states of benzene with principal quantum numbers $n \geq 27$ recorded by monitoring the $C_4H_3^+$ ion fragments. The lower assignment bars indicate Rydberg series of zero quantum defect labeled in the same way as in Fig. 6.

which is significant at the $C_6H_6^+$ mass, is considerably reduced at the fragment masses.

We observe a broadening and a splitting of the lines at low n values which supports the conclusions drawn by Siglow and Neusser that some Rydberg states probed in these experiments have nonzero quantum defects and correspond to the optically accessible Rydberg states.

4. Discussion and conclusions

4.1. Characteristics and range of application of the CRIES technique

The CRIES technique pioneered by Neusser and co-workers [1–6] relies on the observation of unperturbed series of long-lived Rydberg states, and in the case where it has successfully been applied, the Rydberg states were found to have vanishing quantum defects. The experimental results presented in the Section 3 confirm that even the least penetrating optically accessible Rydberg states of benzene, the g states, do not survive the delay times of more than 1 μs between photoexcitation and the application of the pulsed electric field below $n \approx 80$. Optically accessible low-ℓ states of other molecules are very unlikely to be sufficiently long lived to be observed either, and even if they were, interactions between the different ionization channels, and the resulting perturbations in the spectral positions, would make them unsuitable for the CRIES technique. One can therefore conclude that the CRIES technique only works because of Stark mixing of the optically accessible Rydberg states with nonpenetrating high-ℓ states, the mixing simultaneously providing the long lifetimes and suppressing the channel interactions.

The necessity for Stark mixing, however, imposes a condition on the quantum defects of the optically accessible states. The onset of Stark mixing between a Rydberg state of angular momentum quantum number ℓ_i with a quantum defect μ_i and nonpenetrating Rydberg states of higher angular momentum quantum number $\ell \geq \ell_i + 1$ occurs when the separation from the position of zero quantum defect matches the half width of the linear Stark manifold

$$|\mu_i|/n^3 \leq 1.5n^2F \tag{1}$$

In Eq. (1) and in the following, F is given in atomic units, and the value of the quantum defect is constrained to lie between -0.5 and 0.5. Almost complete Stark mixing is observed when the ℓ_i state is fully immersed into the manifold of high-ℓ Stark states, a condition that is fulfilled at approximately twice the field strength given by Eq. (1)

$$2|\mu_i|/n^3 \leq 1.5n^2F \tag{2}$$

Table 1
Minimum (F_{min}) and maximum (F_{max}) values of the electric field required for the observation of resolved transitions to adjacent Stark mixed Rydberg states at representative n values. The quantum defects of the optically accessible states are taken to be 0.1, 0.01, 0.003 and 0.001 in the third, fourth, fifth and sixth columns, respectively

n	F_{max} (V/cm)	F_{min} (V/cm)			
		($\mu_i = 0.1$)	($\mu_i = 0.01$)	($\mu_i = 0.003$)	($\mu_i = 0.001$)
40	8.4	6.7	670	200	67
50	2.7	2.2	220	66	22
60	1.1	0.88	88	27	8.8
70	0.51	0.41	41	12	4.1
80	0.26	0.21	21	6.3	2.1
90	0.15	0.12	12	3.6	1.2
100	0.086	0.069	6.9	2.1	0.69
110	0.053	0.043	4.3	1.3	0.43
120	0.034	0.028	2.8	0.84	0.28
130	0.023	0.018	1.8	0.54	0.18

An additional condition (Eq. (3) below) originates from the fact that transitions to Rydberg states of adjacent n values can only be well resolved if the electric field inducing the Stark mixing is significantly smaller, by at least a factor of 2 assuming that only one series contributes to the spectrum, than the Inglis–Teller field

$$1/(6n^5) \geqslant F. \quad (3)$$

Combining Eqs. (2) and (3) implies that the quantum defect of the optically accessible states must be smaller than 0.125. In addition, Eqs. (2) and (3) give the minimum value F_{min} and the maximum value F_{max} of the stray fields that are compatible with the observation of resolved transitions to long-lived Rydberg states required by the CRIES technique. Together with the quantum defect μ_i of the optically accessible Rydberg states these two conditions determine the range of n values over which a well-resolved Rydberg series can be observed, and Table 1 gives numerical examples for the three values of the quantum defects of 0.1, 0.01, 0.003 and 0.001. For optically accessible states with a quantum defect of 0.1, a resolved series can only be observed over a very narrow range of n values in a given spectrum because the magnitude of F_{min} and F_{max} are comparable (see Table 1). For smaller values of the quantum defect longer series of well-resolved transitions are observable. In the presence of a stray field of approximately 25 mV/cm, for instance, one expects to be able to observe resolved transitions in the range $n = 80$–130, $n = 60$–130 and $n = 50$–130 for series with quantum defects of 0.01, 0.003 and 0.001, respectively.

Conversely, one can obtain an estimate for the quantum defect of the optically accessible series from the range of Rydberg states that are observed experimentally. In their study of benzene, Neuhauser et al. observed Rydberg states from $n \approx 60$ onward in the absence of any intentionally applied electric fields. When a dc electric field of 200 mV/cm was applied, Rydberg series down to $n = 43$ could be observed [1,2]. Using the data in Table 1 one can estimate the quantum defect of the optically accessible series to be approximately 0.003.

These considerations show that the quantum defect of the optically accessible Rydberg series must be significantly less than 0.1 for the CRIES technique to be exploited at its maximum potential. The method therefore promises to function well whenever weakly penetrating Rydberg series with relatively large angular momentum quantum numbers $\ell_i \geq 3$ are optically accessible. In general one-photon excitation schemes from the ground neutral state do not fulfill this requirement. For the technique to be widely applicable, one must therefore be prepared to use multiphoton excitation schemes via intermediate

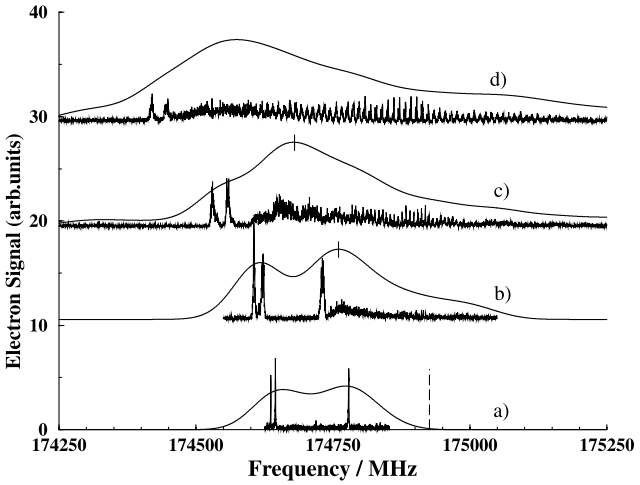

Fig. 9. Effect of weak dc electric fields on the position of the maximum of the intensity distribution of a transition to a weakly penetrating Rydberg state coupled to the nonpenetrating high-ℓ manifold. Above each high-resolution spectrum, synthetic low-resolution spectra obtained by convoluting the spectra with a laser bandwidth of 100 MHz are displayed. Trace a shows transitions from the 77d[3/2]($J = 1$) Rydberg state to the three accessible spin-orbit components of the 91f Rydberg state of the krypton atom. The highest lying component has a quantum defect of 0.017. Traces b, c and d were recorded in the presence of dc electric fields of 10.57 mV/cm, 19.43 mV/cm and 29.45 mV/cm, respectively. The position of zero quantum defect is indicated in the bottom spectrum by a dashed vertical line. The maximum of the intensity distribution of the low resolution spectra is indicated by a vertical mark on the low resolution spectra (b) and (c) and is clearly shifted from the position of zero quantum defect.

states with sufficiently high orbital angular momentum components. Excitation via the S_1 state of benzene and aromatic molecules represents an ideal situation.

4.2. Stark mixing, Stark shifts and systematic errors in the CRIES technique

The Stark mixing that leads to observable series of long-lived Rydberg states can cause an *n*-dependent shift of the line positions that could reduce the accuracy, or even introduce a systematic error in the values of the series limits determined by extrapolation or using the CRIES method. Neuhauser et al. [2] estimated the effect of weak electric fields on the appearance of CRIE spectra of benzene and came to the conclusion that at field strength below 100 mV/cm the shifts were small enough not to cause significant errors in the ionization energies.

The origin of the *n*-dependent shift of the transitions is made apparent in Fig. 9 which illustrates the onset of Stark mixing of the f Rydberg states of krypton with the high-ℓ manifold of Stark states measured at high resolution by millimeter wave spectroscopy. Above each spectrum, a synthetic spectrum has been generated from the experimental data to simulate the effect of a 100 MHz resolution. The quantum defect of the optically accessible 91f[5/2]($J = 2$) state, which is the highest of the three optically accessible spin orbit components seen in the zero field spectrum (Trace a), amounts to 0.017. At the onset of Stark mixing given by Eq. (1), which corresponds approximately to the field present during the recording of Trace b in Fig. 9, the maximum of the intensity distribution is clearly shifted from the position of zero quantum defect marked by a dotted vertical line above Trace a. At electric field strength of 19 mV/cm, corresponding to Eq. (2), the maximum of the intensity distribution is shifted from the position of zero quantum defect by approximately 250 MHz (see vertical mark on Trace c). It is only at fields significantly stronger than those given by Eqs (1) and (2) and used to record the spectra displayed in Fig. 9 that the intensity distribution is centered around the position of zero quantum defect. The shift from the position of zero quantum defect is proportional to the value of the quantum defect μ_i and to n^{-3}. In the case of benzene with an estimated quantum defect of 0.003

(see above) one predicts at $n = 40$ shifts of the order of 520 MHz which corresponds to the width of the lines observed experimentally by Neusser and coworkers. This shift would increase to 5 GHz in a molecule with a quantum defect of 0.03.

4.3. The role of ions in the long-term stabilization of high Rydberg states

The stabilization that results from Stark mixing caused by homogeneous electric fields is sufficient to induce lifetimes longer than the photoexcitation pulses (i.e. $\tau \geq 10$ ns) and thus enables the detection of the Rydberg states by delayed pulsed field ionization. Fig. 2, however, demonstrates that the stabilization is not sufficient for Rydberg states of benzene with n values below ≈ 80 to survive a delay time of more than 1 μs. Instead, one observes a decrease of PFI signal at increasing dc field strength. At the highest n values, this decrease is simply caused by electric field ionization. At intermediate and low n values, the decrease of signal may stem from the coupling, induced by the electric field, between the high ℓ Stark states and successively shorter-lived lower ℓ states starting with the f state. A more important reason for the loss of signal lies in the fact that the m_ℓ mixing that can lead to long-term stability in high Rydberg states becomes less efficient at increasing dc field strength [40,14].

Together, the results presented in Figs 2–5 imply that long-term stabilization (i.e. stabilization to lifetimes longer than 1 μs) cannot be induced in benzene Rydberg states below $n \approx 80$ by homogeneous electric fields, but can be reached by generating a sufficient concentration of ions in the experimental volume. This stabilization by ions only affects a very small fraction of the initially prepared Rydberg states at the lowest n values, but this fraction grows continuously with increasing n values (see Fig. 6). The field ionization characteristics of the long-lived states indicate that the stabilization does not result from n changing processes. The overall features of our experimental results on the stabilization of high Rydberg states by ions can be described as follows

1. Noticeable stabilization only occurs when the average field of the ion distribution, as given by Holtsmark's formula [42–44], is large enough to satisfy Eq. (1) a condition that can be expressed by

$$(9.14 \times 10^{15}|\mu_i|/n^5)^{3/2} \leq c/\ (\text{ions/cm}^3) \qquad (4)$$

which relates the n value and the quantum defect μ_i of the optically accessible Rydberg state to the ion concentration required to achieve stabilization. Table 2 gives numerical values of the predicted ion concentrations necessitated to stabilize Rydberg states of quantum defects μ_i of 0.003, 0.01 and 0.03 at representative n values. Eq. (4) simply requires that the average field of the ion distribution is large enough to induce appreciable Stark mixing. The fact that a homogeneous electric field of the same magnitude does not suffice to stabilize the Rydberg states beyond 1 μs below $n = 80$ (see above) implies that the role of the ions cannot be reduced to that of a homogeneous field. In particular, the electric field of a distribution of charged particles can induce m_ℓ mixing [13,14].
2. Stabilization does not affect all Rydberg states equally. Only a fraction of the prepared Rydberg states are detected by delayed pulsed field ionization at delays longer than 1 μs. This fraction, which is almost independent of the delay for delays beyond 1 μs (see Fig. 4), amounts to only around 1% at the lowest n values for which Eq. (4) is fulfilled ($n = 40$ in Fig. 6) and reaches values of

Table 2
Ion concentrations necessitated to stabilize Rydberg states of quantum defects μ_i of 0.03, 0.01 and 0.003 at representative n values

n	c (ions/cm^3)		
	($\mu_i = 0.03$)	($\mu_i = 0.01$)	($\mu_i = 0.003$)
40	4.4×10^9	8.4×10^8	1.4×10^8
50	8.2×10^8	1.6×10^8	2.6×10^7
60	2.1×10^8	4.0×10^7	6.6×10^6
70	6.6×10^7	1.3×10^7	2.1×10^6
80	2.4×10^7	4.7×10^6	7.7×10^5
90	1.0×10^7	1.9×10^6	3.2×10^5
100	4.5×10^6	8.7×10^5	1.4×10^5
110	2.2×10^6	4.3×10^5	7.0×10^4
120	1.2×10^6	2.2×10^5	3.7×10^4
150	2.2×10^5	4.2×10^4	6.8×10^3
200	2.5×10^4	4.8×10^3	7.9×10^2
400	140	27	4

typically 10–30% at ion concentrations where the average electric field of the ion distribution satisfies Eq. (2) ($n \geq 50$ Fig. 6). This observation is in qualitative agreement with recent calculations by Softley and Rednall which show that m_ℓ mixing is only substantial at very specific configurations of the ions around the Rydberg molecules [18]. It also explains the almost stochastic and nonreproducible appearance of the spectral features at the lowest laser fluences (see for instance Fig. 3a).

3. The ion concentrations that are required to observe long-lived states in benzene at n values below 80 are large ($\approx 10^6$ ions/cm^3 at $n = 80$; $\approx 10^8$ ions/cm^3 at $n = 40$) and would be even larger in other molecular systems in which the quantum defects of the optically accessible Rydberg series are larger. However, Table 2 also illustrates that much smaller concentrations are required to achieve long-term stability at the high n values ($n \geq 200$) probed in PFI-ZEKE photoelectron spectroscopic experiments.

References

[1] R. Neuhauser, H.J. Neusser, Chem. Phys. Lett. 253 (1996) 151.
[2] R.G. Neuhauser, K. Siglow, H.J. Neusser, J. Chem. Phys. 106 (1997) 896.
[3] K. Siglow, H.J. Neusser, J. Chem. Phys. 112 (2000) 647.
[4] K. Siglow, R. Neuhauser, H.J. Neusser, Chem. Phys. Lett. 293 (1998) 19.
[5] K. Siglow, R. Neuhauser, H.J. Neusser, J. Chem. Phys. 110 (1999) 5589.
[6] K. Siglow, H.J. Neusser, Faraday Discuss. 115 (2000) 245.
[7] M. Oldani, R. Widmer, G. Grassi, A. Bauder, J. Mol. Struct. 190 (1988) 31.
[8] T. Brupbacher, A. Bauder, Chem. Phys. Lett. 173 (1990) 435.
[9] T. Brupbacher, J. Makarewicz, A. Bauder, J. Chem. Phys. 101 (1994) 9736.
[10] A. Bauder, J. Mol. Struct. 408 (1997) 33.
[11] E. Miescher, K.P. Huber, in: D.A. Ramsey (Ed.), International Review of Science, Physical Chemistry Series 2, vol. 3, 1976, p. 37.
[12] C.H. Herzberg, G. Jungen, J. Mol. Spectrosc. 41 (1972) 425.
[13] W.A. Chupka, J. Chem. Phys. 98 (1993) 4520.
[14] F. Merkt, R. Zare, J. Chem. Phys. 101 (1994) 3495.
[15] M.J.J. Vrakking, J. Phys. Chem. A 101 (1997) 6761.
[16] J.D.D. Martin, J.W. Hepburn, C. Alcaraz, J. Phys. Chem. A 101 (1997) 6728.
[17] A. Held, E.W. Schlag, Laser Chem. 18 (1998) 13.
[18] T.P. Softley, R.J. Rednall, J. Chem. Phys. 112 (2000) 7992.
[19] S.R. Procter, M.J. Webb, T.P. Softley, Faraday Discuss. 115 (2000) 277.
[20] H.J. Neusser, General discussion, Faraday Discuss. 115 (2000) 313.
[21] L.A. Chewter, M. Sander, K. Müller-Dethlefs, E.W. Schlag, J. Chem. Phys. 86 (1987) 4737.
[22] I. Fischer, R. Lindner, K. Müller-Dethlefs, J. Chem. Soc., Faraday Trans. 90 (1994) 2425.
[23] R. Lindner, H.-J. Dietrich, K. Müller-Dethlefs, Chem. Phys. Lett. 228 (1994) 417.
[24] C. Alt, W.G. Scherzer, H.L. Selzle, E.W. Schlag, Chem. Phys. Lett. 240 (1995) 457.
[25] H.-J. Dietrich, K. Müller-Dethlefs, L. Ya. Baranov, Phys. Rev. Lett. 76 (1996) 3530.
[26] P.M. Johnson, J. Chem. Phys. 64 (1976) 4143.
[27] M. Allan, Helv. Chim. Acta 65 (1982) 2008.
[28] J.M. Wiesenfeld, B.I. Greene, Phys. Rev. Lett. 51 (1983) 1745.
[29] R.L. Whetten, K.-J. Fu, E.R. Grant, J. Chem. Phys. 79 (1983) 2626.
[30] S.G. Grubb, C.E. Otis, R.L. Whetten, E.R. Grant, A.C. Albrecht, J. Chem. Phys. 82 (1985) 1135.
[31] R.L. Whetten, S.G. Grubb, C.E. Otis, A.C. Albrecht, E.R. Grant, J. Chem. Phys. 82 (1985) 1115.
[32] W.A. Chupka, J. Chem. Phys. 99 (1993) 5800.
[33] F. Merkt, H. Schmutz, J. Chem. Phys. 108 (1998) 10033.
[34] F. Merkt, R. Signorell, H. Palm, A. Osterwalder, M. Sommavilla, Mol. Phys. 95 (1998) 1045.
[35] A. Osterwalder, F. Merkt, Phys. Rev. Lett. 82 (1999) 1831.
[36] A. Osterwalder, R. Seiler, F. Merkt, J. Chem. Phys. 113 (2000) 7939.
[37] S. Gerstenkorn, P. Luc, J. Verges, Atlas du Spectre d'Absorption de la Molécule d'Iode, CNRS, Orsay, 1993.
[38] F. Merkt, Ann. Rev. Phys. Chem. 48 (1997) 675.
[39] S.T. Pratt, J. Chem. Phys 98 (1993) 9241.
[40] F. Merkt, J. Chem. Phys. 100 (1994) 2623.
[41] H.-J. Dietrich, R. Lindner, K. Müller-Dethlefs, J. Chem. Phys. 101 (1994) 3399.
[42] J. Holtsmark, Ann. Phys. 58 (1919) 577.
[43] J. Holtsmark, Phys. Z. 25 (1924) 73.
[44] H. Palm, R. Signorell, F. Merkt, Phil. Trans. R. Soc. Lond. A 355 (1997) 1551.